Electronic Supplementary information for

Rotors tailoring molecular stacking for constructing multi-stimuli-responsive luminescent materials

Zheng-Fei Liu, Lan Zeng, Li-Ya Niu and Qing-Zheng Yang*

Key Laboratory of Radiopharmaceuticals, Ministry of Education, College of Chemistry, Beijing Normal University, Beijing 100875, P. R. China.

Email: qzyang@bnu.edu.cn

Table of Content

1. Materials

General reagents and solvents were purchased from commercial suppliers and used without any purification, unless otherwise noted, 2-acetyl pyrrole, iodoethane, 2-iodothiophene, methyl 1*H*-pyrrole-2-carboxylate, boron trifluoride diethyl etherate, triethylamine, cesium carbonate, potassium hydroxide, copper powder and sodium hydride were purchased from Sun Chemical Technology (Shanghai) Co. Ltd. All solvents were purchased from Beijing Chemical Reagent Plant.

2. Characterization methods

2.1 Nuclear magnetic resonance (NMR)

Nuclear magnetic resonance (NMR) spectra were recorded on JEOL-600 spectrometer at room temperature. Chemical shift values (δ) and coupling constants (J) are reported in ppm and Hertz (Hz), respectively. The signals multiplicity for ^{1}H NMR spectra are described using the following abbreviations: "s" (singlet), "d" (doublet), "t" (triplet), "dt" (doublet of triplets), "dd" (doublet of doublets) and "m" (multiplet).

2.2 Electrospray ionization mass spectroscopy (ESI-MS)

High-resolution mass spectrometry experiments were performed on Bruker Solarix XR Fourier Transform Ion Cyclotron Resonance Mass Spectrometer.

2.3 Single crystal X-ray diffraction (SC-XRD)

Single crystal X-ray diffraction (SC-XRD) data were collected on a SuperNova Rigaku Oxford Diffraction diffractometer with Cu-Kα radiation, λ = 1.54184 Å. NoSpherA2, an implementation of NOn-SPHERical Atom-form-factors in Olex2 was used for refinement of the crystal structures.[1] The crystal structure data are summarized in Table S1-S2.

2.4 UV-Vis absorption and photoluminescence spectroscopy

UV–visible absorption and emission spectra for the solution samples were recorded with Hitachi UV-3900 and F-4600 spectrometer, respectively. Steady fluorescence spectra of solid samples were determined by Edinburgh instruments FLS-980. The time resolved fluorescence spectra were recorded by time-correlated single photon counting Edinburgh Instruments FLS-980. Fluorescence quantum yields were determined on HAMAMATSU C11347.

2.5 Powder X-ray diffraction (PXRD)

PXRD patterns were measured by Shimadzu XRD-7000 with Cu-Kα radiation (λ = 1.54050 Å) operated in the 2θ range from 5 to 40°.

2.6 Theoretical calculations

All calculations were performed with the Gaussian09 program.[2] Single-point calculations are done with the simplified TD-DFT based on electronic wavefunctions calculated at the B3LYP level. DFT calculated minimum-energy isomerization pathway along the rotation of the N−C bond between the pyrrole and thiophene ring, using 1° per step. The 6-311G basis sets are used in all calculations.

3. Synthesis
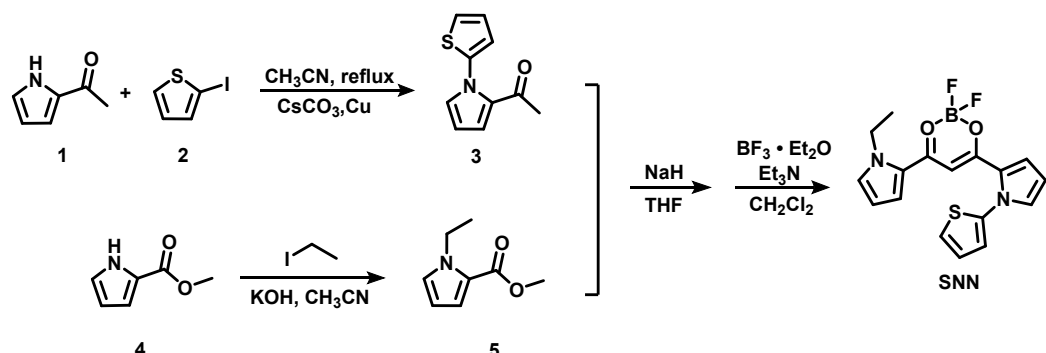
Figure S1. Synthetic route of **SNN**.

Synthesis of 1-(1-(thiophen-2-yl)-1*H*-pyrrol-2-yl)ethan-1-one (compound 3):

The synthesis of compound **3** refer to the reported literature.[3]

Synthesis of methyl 1-ethyl-1*H*-pyrrole-2-carboxylate (compound 5): To a solution of methyl 1*H*-pyrrole-2-carboxylate (500.0 mg, 4.0 mmol) in 50.0 mL acetonitrile was added potassium hydroxide (771.0 mg, 13.7 mmol) and iodoethane (1.3 g, 8.3 mmol). The reaction mixture was stirred at room temperature for 2 hours. The resulting mixture was extracted with dichloromethane (3× 30.0 mL) and the organic phase was collected, dried over anhydrous sodium sulfate and concentrated in vacuum. The crude product was purified by column chromatography (petroleum ether/dichloromethane = 3:1) to yield compound **5** (520.0 mg, 85%) as a light-yellow oil. ^{1}H NMR (600 MHz, CDCl$_3$) δ 7.05 – 6.91 (m, 1H), 6.85 (s, 1H), 6.18 – 5.98 (m, 1H), 4.35 (q, J = 7.2 Hz, 2H), 3.80 (s, 2H), 1.38 (t, J = 7.2 Hz, 2H).

Synthesis of SNN:

Step 1: Compound **3** (300.0 mg, 1.6 mmol) and THF (5.0 mL) were added to a 25.0 mL round-bottom flask and purged with nitrogen for 10 mins. Then NaH (57-63% oil dispersion, 188.0 mg, 4.7 mmol) was added to the resultant solution, and stirred under nitrogen at 60 °C for 30 min, followed by slow addition of compound **5** (350.0 mg, 1.6 mmol). The resulting mixture was refluxed under nitrogen for 20 hours. The reaction mixture was allowed to cool to room temperature before being quenched carefully with water (10.0 mL) in ice bath. The pH was adjusted to 3 with HCl (aq). The aqueous

suspension was extracted with dichloromethane (3× 30.0 mL). The organic phase was dried over anhydrous sodium sulfate, and concentrated under reduced pressure to obtain the crude product as a brown oil. The crude product was directly used for next step without further purification.

Step 2: To a solution of the crude product in 10.0 mL dichloromethane was added 1.0 mL Et_3N. After stirring for 10 min at room temperature, 1.0 mL $BF_3 \cdot Et_2O$ was added. The solution was stirred for another 2 hours in the dark. Water was added to the solution, and the organic layers was collected, washed with water, dried over anhydrous sodium sulfate, and concentrated under reduced pressure. The crude product was purified by column chromatography (petroleum ether/dichloromethane = 1:1) to yield **SNN** (265.0 mg, 46%) as a yellow solid. ^1H NMR (600 MHz, $CDCl_3$, 298 K) δ 7.40 (d, J = 5.5 Hz, 1H), 7.38 (dd, J = 4.0, 1.4 Hz, 1H), 7.26 (s, 1H), 7.13 (q, J = 3.1, 2.5 Hz, 3H), 7.11 (dd, J = 5.3, 3.9 Hz, 1H), 7.03 (s, 1H), 6.64 – 6.58 (m, 1H), 6.45 – 6.41 (m, 1H), 6.19 (dd, J = 4.1, 2.5 Hz, 1H), 5.88 (s, 1H), 4.37 (q, J = 7.2 Hz, 2H), 1.56 (s, 2H), 1.42 (t, J = 7.2 Hz, 3H). ^{13}C NMR (151 MHz, $CDCl_3$, 298 K) δ 172.28, 168.41, 140.89, 134.44, 133.52, 129.75, 126.01, 125.90, 125.38, 122.29, 121.54, 111.50, 111.02, 92.52, 46.27, 16.94, 0.06. HR-MS (ESI) $C_{17}H_{16}BF_2N_2O_2S^+$ $[M+H]^+$, Calculated: 361.0991; Found: 361.0990.

Preparation of PMMA Films doped with different concentration of SNN: The **SNN** and PMMA with different mass ratios were dissolved in 1-2 mL dichloromethane. The clear solutions were deposited on optical grade quartz plates of 1x1 cm by drop casting, and allowed to dry 1 hour.

## 4. The absorption and emission spectra in solution
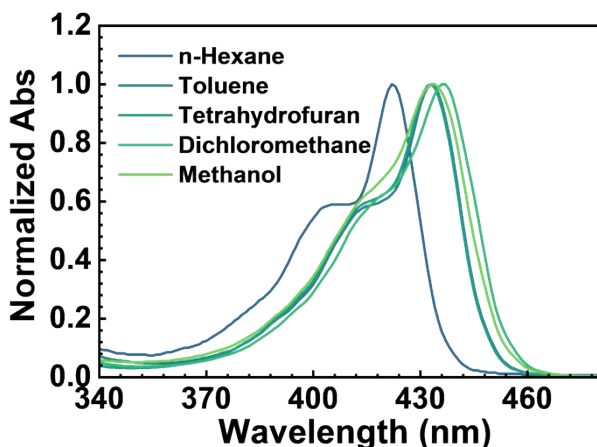
Figure S2. The normalized absorption spectra of **SNN** in different solvents (1×10^{-5} M).
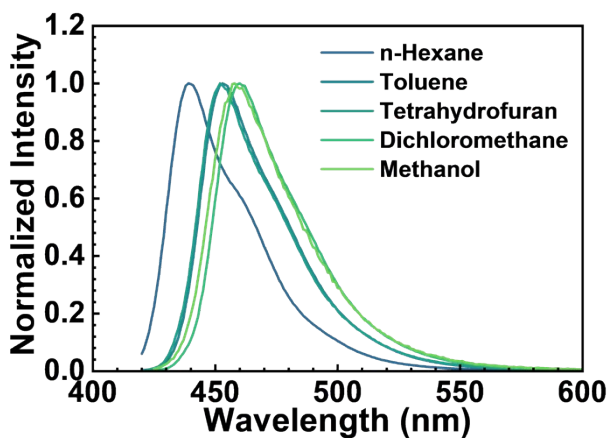

Figure S3. The normalized fluorescence spectra of **SNN** in different solvents (1×10^{-5} M).

5. X-ray crystallography

The **G** and **O** of **SNN** suitable for X-ray crystallography were obtained by slow evaporation of its solution in mixed solvents of dichloromethane and *n*-hexane (v/v = 1:1). CCDC deposition numbers of **G** and **O** are 2224763 and 2224926 respectively.

Table S1. Crystal data and structure refinement for **G**.

Identification code	**G**
Empirical formula	$C_{17}H_{15}BF_2N_2O_2S$
Formula weight	360.18
Temperature	100.01(10) K
Wavelength	1.54184 Å
Crystal system, space group	triclinic, $P\bar{1}$
Unit cell dimensions	$a = 7.3035(2)$ Å, $\alpha = 76.416(2)°$
	$b = 9.1624(3)$ Å, $\beta = 89.655(2)°$
	$c = 12.5664(3)$ Å, $\gamma = 79.328(2)°$
Volume	802.63(4) Å^3
Z, Calculated density	2, 1.490 g/cm^3
Absorption coefficient	2.118 mm^{-1}
F (000)	372.0
Crystal size	$0.2 \times 0.2 \times 0.1$ mm^3
2θ range for data collection	7.24 to 152.64°
Index ranges	-9 <= h <= 8, -11 <= k <= 11, -15 <= l <= 14
Reflections collected	8646
Independent reflections	3028 [$R_{int} = 0.0257$, $R_{sigma} = 0.0259$]
Data/restraints/parameters	3208/0/362
Goodness-of-fit on F^2	1.046
Final R indexes [I>=2σ (I)]	$R_1 = 0.0327$, $wR_2 = 0.0858$
Final R indexes [all data]	$R_1 = 0.0336$, $wR_2 = 0.0865$
Largest diff. peak/hole / e	0.30/-0.24 Å^{-3}

Table S2. Crystal data and structure refinement for **O**.

Identification code	**O**
Empirical formula	$C_{17}H_{15}BF_2N_2O_2S$
Formula weight	360.208
Temperature	100.15 K
Wavelength	1.54184 Å
Crystal system, space group	triclinic, $P\bar{1}$
Unit cell dimensions	$a = 8.4059(2)$ Å, $\alpha = 109.969(2)°$
	$b = 9.7970(2)$ Å, $\beta = 99.326(2)°$
	$c = 11.4192(2)$ Å, $\gamma = 104.781(2)°$
Volume	$821.86(4)$ Å^3
Z, Calculated density	2, 1.456 g/cm^3
Absorption coefficient	2.069 mm^{-1}
F (000)	374.0
Crystal size	$0.2 \times 0.2 \times 0.2$ mm^3
2θ range for data collection	8.56 to 153.08°
Index ranges	$-10 <= h <= 10, -12 <= k <= 12, -13 <= l <= 14$
Reflections collected	8864
Independent reflections	3278 [$R_{int} = 0.0254$, $R_{sigma} = 0.0237$]
Data/restraints/parameters	3278/187/348
Goodness-of-fit on F^2	1.092
Final R indexes [I>=2σ (I)]	$R_1 = 0.0263$, $wR_2 = 0.0702$
Final R indexes [all data]	$R_1 = 0.0273$, $wR_2 = 0.0708$
Largest diff. peak/hole / e	0.24/-0.24

Table S3. Anisotropic Displacement Parameters ($Å^2×10^3$) for **G**. The Anisotropic displacement factor exponent takes the form: $-2\pi^2[h^2a^{*2}U_{11}+2hka^*b^*U_{12}+\ldots]$.

Atom	U_{11}	U_{22}	U_{33}	U_{12}	U_{13}	U_{23}
S16	17.92(19)	13.37(18)	23.4(2)	-1.56(13)	2.33(13)	-2.05(12)
F25	15.3(4)	31.6(5)	18.5(4)	-6.0(3)	2.1(3)	-5.2(3)
F24	34.8(5)	16.4(4)	20.0(4)	-4.3(3)	1.4(3)	-0.5(3)
O2	12.6(4)	23.5(5)	14.7(5)	-5.1(4)	0.0(3)	0.1(4)
O4	14.2(4)	22.6(5)	14.2(4)	-4.2(4)	0.9(3)	0.8(4)
N11	14.2(5)	13.1(5)	12.8(5)	-3.4(4)	0.6(4)	-1.3(4)
N21	19.5(6)	20.8(6)	13.0(5)	-2.6(4)	-0.5(4)	-3.6(4)
C1	13.5(6)	10.8(6)	16.8(6)	-4.4(5)	1.8(5)	-2.5(4)
C10	20.1(6)	15.7(6)	12.3(6)	-3.8(5)	2.7(5)	-4.6(5)
C20	17.7(6)	16.1(6)	14.2(6)	-3.2(5)	1.0(5)	-3.4(5)
C12	16.6(6)	13.8(6)	12.4(6)	-4.1(5)	1.7(5)	-0.9(5)
C6	14.2(6)	16.2(6)	14.6(6)	-3.1(5)	0.6(5)	-1.1(5)
C7	14.4(6)	12.9(6)	14.8(6)	-4.4(5)	0.8(5)	-2.5(5)
C9	21.9(7)	14.9(6)	12.7(6)	-2.6(5)	-0.7(5)	-3.4(5)
C5	15.3(6)	10.9(6)	17.0(6)	-3.6(5)	0.6(5)	-2.5(5)
C8	16.1(6)	13.9(6)	16.4(6)	-4.2(5)	-1.0(5)	-1.9(5)
C13	17.6(6)	17.4(6)	17.3(6)	-6.5(5)	-0.3(5)	-2.1(5)
C22	20.6(7)	30.7(8)	13.5(6)	-6.4(5)	4.2(5)	-6.0(6)
C19	18.4(6)	20.3(7)	17.9(7)	-2.6(5)	-1.1(5)	-0.7(5)
C14	16.7(6)	25.0(7)	19.6(7)	-6.6(6)	-1.9(5)	2.5(5)
C15	21.2(7)	19.5(7)	19.2(7)	-1.9(5)	2.2(5)	3.7(5)
C17	26.3(7)	26.0(7)	13.8(6)	-1.4(5)	-4.9(5)	-5.7(6)
C18	22.0(7)	25.2(7)	21.4(7)	-1.9(6)	-6.6(6)	-1.0(6)
C23	24.2(7)	28.1(8)	22.6(7)	-12.2(6)	3.7(6)	-1.8(6)
B3	14.8(7)	16.8(7)	13.6(7)	-3.7(5)	0.2(5)	0.1(5)

Table S4. Anisotropic Displacement Parameters ($Å^2×10^3$) for **O**. The Anisotropic displacement factor exponent takes the form: $-2\pi^2[h^2a^{*2}U_{11}+2hka^*b^*U_{12}+…]$.

Atom	U_{11}	U_{22}	U_{33}	U_{12}	U_{13}	U_{23}
S1	21.4(3)	36.3(2)	24.9(2)	10.2(2)	6.5(2)	10.20(16)
F002	60.1(4)	28.9(3)	31.2(3)	22.0(3)	17.5(3)	17.1(3)
F003	43.6(4)	27.0(3)	30.6(3)	0.6(3)	19.1(3)	6.0(2)
O004	36.1(4)	20.2(3)	23.0(3)	10.9(3)	14.4(3)	10.6(3)
O005	46.0(4)	25.6(3)	30.3(4)	17.8(3)	22.8(3)	15.4(3)
C10	25.4(11)	28.8(8)	27.5(7)	9.1(5)	8.7(4)	11.8(4)
N007	22.8(4)	18.7(4)	22.7(4)	6.5(3)	7.0(3)	6.6(3)
C008	22.6(4)	17.2(4)	19.7(4)	4.8(3)	6.7(3)	7.3(3)
C009	23.0(4)	18.1(4)	23.2(4)	5.9(3)	7.3(3)	8.5(3)
N8	21.4(11)	24.7(9)	20.1(9)	2.9(7)	7.4(8)	2.6(7)
C00B	24.4(4)	20.5(4)	21.1(4)	5.4(3)	10.2(3)	8.2(3)
C00C	24.4(4)	25.6(5)	20.6(4)	6.2(4)	9.7(3)	7.8(4)
C00D	28.9(5)	21.1(4)	20.1(4)	7.7(4)	8.3(4)	9.0(4)
H00D	80(12)	31(8)	46(9)	27(8)	24(8)	19(7)
C00E	28.1(5)	19.1(4)	32.2(5)	9.0(4)	9.1(4)	6.6(4)
H00E	69(12)	39(9)	47(9)	19(8)	27(8)	16(8)
C00F	31.2(5)	22.1(5)	29.6(5)	8.8(4)	8.8(4)	13.7(4)
H00F	71(11)	42(9)	28(8)	30(8)	20(7)	19(7)
C00G	34.2(5)	21.2(5)	38.4(6)	11.1(4)	9.9(4)	14.3(4)
H00G	59(11)	42(9)	62(10)	25(8)	9(8)	31(8)
C00H	22.9(4)	21.9(4)	21.0(4)	7.6(3)	9.0(3)	6.6(3)
C00I	41.2(19)	41(2)	24.7(14)	14.9(15)	16.2(13)	16.5(15)
C00J	31(2)	46(2)	17.1(15)	8.2(12)	9.2(12)	8.2(10)
C00K	41.2(18)	43(2)	25.6(12)	22.7(17)	12.3(13)	14.5(13)
C00L	26(2)	35.2(13)	18.4(11)	5.6(12)	6.8(12)	9.3(9)
C00M	19(2)	36.0(15)	21.8(13)	2.3(11)	5.7(12)	1.7(10)
B1	36.9(6)	19.5(5)	25.6(5)	9.3(4)	15.7(4)	11.1(4)
C00O	27.2(8)	24.6(8)	31.8(8)	6.9(6)	12.8(6)	7.6(6)
C00P	40.4(10)	23.2(9)	52.6(11)	4.8(7)	22.7(8)	10.1(8)

S1a	23.9(13)	33.1(9)	28.9(8)	10.9(8)	10.3(7)	14.0(6)
C10a	12(4)	35(3)	30(3)	2(2)	3(2)	10.3(17)
C1	26(4)	35(6)	28(6)	10(3)	7(2)	10(3)
C2	23(4)	23(4)	30(6)	11(2)	9(2)	8(3)
N8a	22(2)	21.3(17)	18.9(16)	6.7(13)	5.1(13)	2.0(12)
C3	36(6)	35(3)	22(3)	14(3)	11(2)	10.2(18)
C4	29(5)	24(2)	19(2)	7(2)	8(2)	9.3(15)
C00n	18(4)	27(3)	16(2)	7(2)	3.0(18)	0.8(15)
C5	26.1(15)	21.4(15)	30.1(16)	8.3(11)	8.0(11)	4.8(11)
C00q	29.4(17)	45(2)	47(2)	13.7(14)	12.4(13)	25.0(15)

Table S5. Bond Lengths for **G**.

Atom	Atom	Length/Å	Atom	Atom	Length/Å
S16	C12	1.7279(13)	C1	C6	1.3816(18)
S16	C15	1.7193(15)	C1	C7	1.4442(18)
F25	B3	1.3702(17)	C10	C9	1.3748(19)
F24	B3	1.3859(17)	C20	C5	1.4296(18)
O2	C1	1.3217(15)	C20	C19	1.3985(19)
O2	B3	1.4757(16)	C12	C13	1.3534(19)
O4	C5	1.3099(16)	C6	C5	1.4017(18)
O4	B3	1.4829(17)	C7	C8	1.3878(18)
N11	C10	1.3700(16)	C9	C8	1.4046(18)
N11	C12	1.4184(16)	C13	C14	1.4253(19)
N11	C7	1.3950(16)	C22	C23	1.520(2)
N21	C20	1.3902(17)	C19	C18	1.394(2)
N21	C22	1.4738(18)	C14	C15	1.356(2)
N21	C17	1.3551(18)	C17	C18	1.382(2)

Table S6. Bond Lengths for **O**.

Atom	Atom	Length/Å	Atom	Atom	Length/Å
S1	C00H	1.7210(11)	C00B	C00D	1.3929(13)
S1	C00K	1.711(5)	C00C	C00L	1.392(5)
F002	B1	1.3645(13)	C00C	N8a	1.430(4)
F003	B1	1.3878(13)	C00C	C4	1.399(9)
O004	C008	1.3050(11)	C00E	C00G	1.3813(15)
O004	B1	1.4773(12)	C00F	C00G	1.4082(14)
O005	C00B	1.3068(11)	C00H	S1a	1.657(3)
O005	B1	1.4822(12)	C00H	C10a	1.355(9)
C10	C00H	1.381(3)	C00I	C00K	1.364(6)
C10	C00I	1.415(6)	C00J	C00L	1.394(8)
N007	C009	1.3939(11)	C00J	C00M	1.399(11)
N007	C00E	1.3669(12)	C00O	C00P	1.523(2)
N007	C00H	1.4130(12)	S1a	C2	1.71(2)
C008	C009	1.4387(12)	C10a	C1	1.46(2)
C008	C00D	1.3933(12)	C1	C2	1.38(3)
C009	C00F	1.3937(13)	N8a	C00n	1.340(9)
N8	C00C	1.376(3)	N8a	C5	1.473(6)
N8	C00M	1.360(5)	C3	C4	1.416(15)
N8	C00O	1.463(3)	C3	C00n	1.368(17)
C00B	C00C	1.4348(12)	C5	C00q	1.513(5)

Table S7. Bond Angles for **G**.

Atom	Atom	Atom	Angle/°	Atom	Atom	Atom	Angle/°
C15	S16	C12	90.82(7)	C8	C7	N11	107.08(11)
C1	O2	B3	121.76(10)	C8	C7	C1	126.19(12)
C5	O4	B3	121.91(11)	C10	C9	C8	107.28(12)
C10	N11	C12	122.79(11)	O4	C5	C20	117.13(12)
C10	N11	C7	108.53(10)	O4	C5	C6	120.87(12)
C7	N11	C12	127.90(11)	C6	C5	C20	122.00(12)
C20	N21	C22	129.09(11)	C7	C8	C9	108.12(12)
C17	N21	C20	108.11(12)	C12	C13	C14	111.67(12)
C17	N21	C22	122.51(12)	N21	C22	C23	112.70(11)
O2	C1	C6	121.38(12)	C18	C19	C20	107.77(13)
O2	C1	C7	112.19(11)	C15	C14	C13	113.00(12)
C6	C1	C7	126.39(12)	C14	C15	S16	111.94(11)
N11	C10	C9	108.98(11)	N21	C17	C18	109.82(12)
N21	C20	C5	124.89(12)	C17	C18	C19	106.88(12)
N21	C20	C19	107.41(12)	F25	B3	F24	111.09(11)
C19	C20	C5	127.70(12)	F25	B3	O2	108.89(11)
N11	C12	S16	120.02(10)	F25	B3	O4	108.42(11)
C13	C12	S16	112.54(10)	F24	B3	O2	108.91(11)
C13	C12	N11	127.32(12)	F24	B3	O4	108.20(11)
C1	C6	C5	119.46(12)	O2	B3	O4	111.34(11)
N11	C7	C1	126.33(11)				

Table S8. Bond Angles for **O**.

Atom	Atom	Atom	Angle/°	Atom	Atom	Atom	Angle/°
C00K	S1	C00H	91.2(2)	C10	C00H	S1	111.16(12)
B1	O004	C008	120.29(7)	N007	C00H	S1	120.43(7)
B1	O005	C00B	120.45(8)	N007	C00H	C10	128.40(13)
C00I	C10	C00H	113.0(3)	S1a	C00H	S1	120.14(11)
C00E	N007	C009	108.43(8)	S1a	C00H	C10	8.98(18)
C00H	N007	C009	128.07(7)	S1a	C00H	N007	119.43(11)
C00H	N007	C00E	123.04(8)	C10a	C00H	S1	4.9(5)
C009	C008	O004	116.83(8)	C10a	C00H	C10	106.3(5)
C00D	C008	O004	121.36(8)	C10a	C00H	N007	125.3(5)
C00D	C008	C009	121.79(8)	C10a	C00H	S1a	115.3(5)
C008	C009	N007	124.19(8)	C00K	C00I	C10	111.3(5)
C00F	C009	N007	107.43(8)	C00M	C00J	C00L	107.0(6)
C00F	C009	C008	128.27(8)	C00I	C00K	S1	113.2(4)
C00M	N8	C00C	107.8(3)	C00J	C00L	C00C	107.0(5)
C00O	N8	C00C	130.47(18)	C00J	C00M	N8	109.1(5)
C00O	N8	C00M	121.7(3)	F003	B1	F002	111.52(8)
C00C	C00B	O005	117.65(8)	O004	B1	F002	109.17(8)
C00D	C00B	O005	120.61(8)	O004	B1	F003	108.49(8)
C00D	C00B	C00C	121.70(9)	O005	B1	F002	108.92(8)
C00B	C00C	N8	124.57(12)	O005	B1	F003	108.17(8)
C00L	C00C	N8	109.0(3)	O005	B1	O004	110.57(8)
C00L	C00C	C00B	126.4(3)	C00P	C00O	N8	113.23(18)
N8a	C00C	N8	20.52(14)	C2	S1a	C00H	88.6(8)
N8a	C00C	C00B	125.8(2)	C1	C10a	C00H	113.4(11)
N8a	C00C	C00L	104.9(3)	C2	C1	C10a	104.9(19)
C4	C00C	N8	103.5(4)	C1	C2	S1a	117.6(19)
C4	C00C	C00B	129.5(4)	C00n	N8a	C00C	109.2(5)
C4	C00C	C00L	14.1(5)	C5	N8a	C00C	128.7(3)
C4	C00C	N8a	104.5(5)	C5	N8a	C00n	122.1(5)
C00B	C00D	C008	119.06(9)	C00n	C3	C4	106.1(12)

|							
C00G	C00E	N007	109.28(9)	C3	C4	C00C	109.3(8)
C00G	C00F	C009	107.78(9)	C3	C00n	N8a	110.6(10)
C00F	C00G	C00E	107.08(9)	C00q	C5	N8a	112.4(4)

6. Theoretical calculations
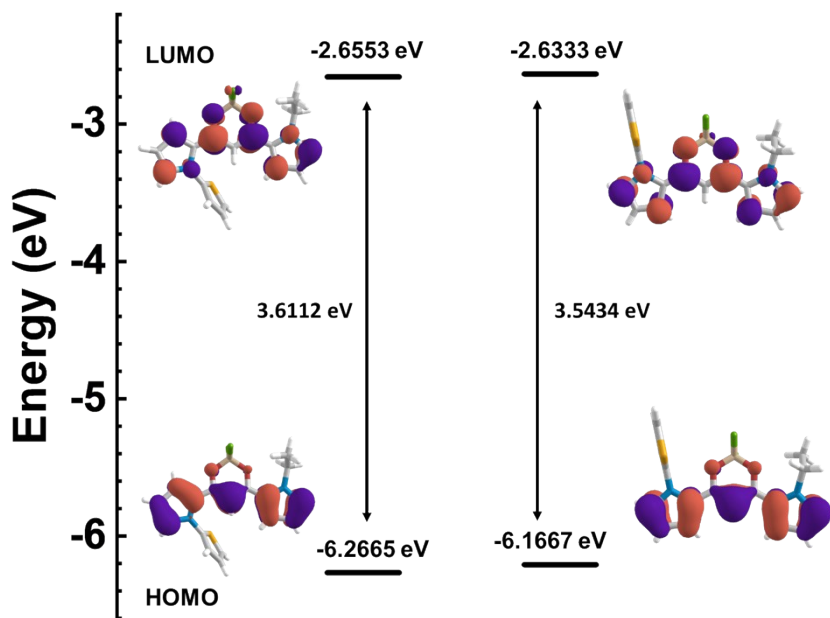
Figure S4. Frontier molecular orbitals (HOMO and LUMO) of the monomers selected in **G** (left) and **O** (right) respectively.
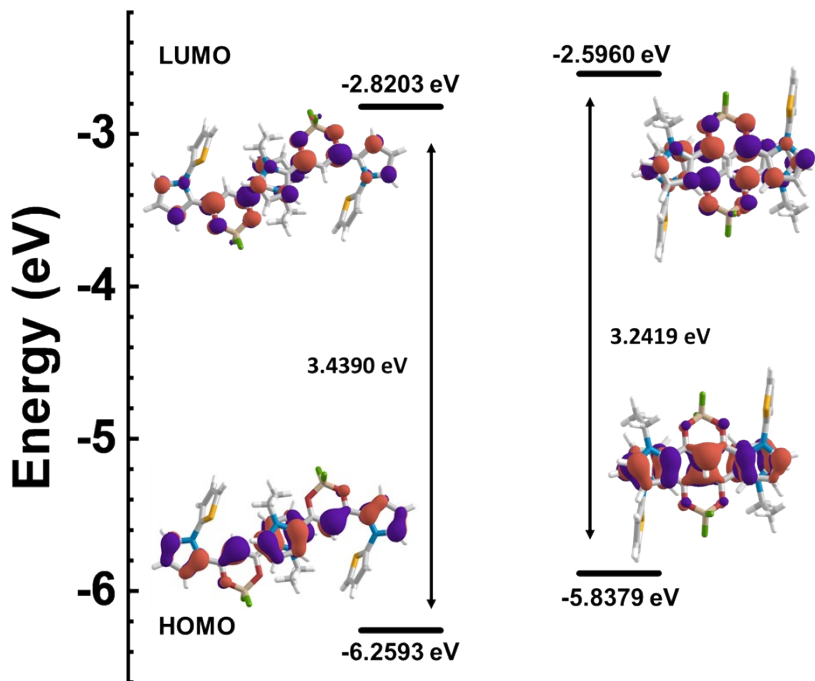

Figure S5. Frontier molecular orbitals (HOMO and LUMO) of the stacking dimers selected in **G** (left) and **O** (right) respectively.
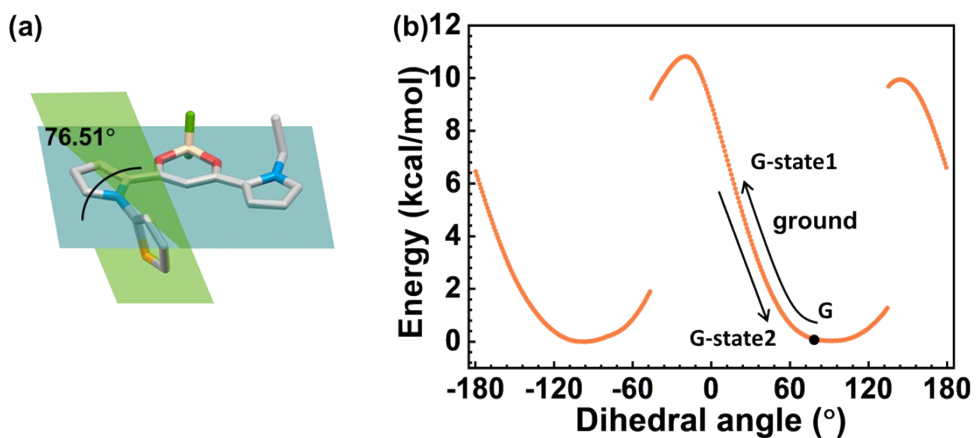
Figure S6. (a) Dihedral angle between the thiophene ring and conjugated body of **SNN** in **G**. (b) Potential energy landscape along the rotation of the thiophene ring of **SNN**.

7. The analysis of crystal structures

(a) π-π

3.5173(1) Å

3.3526(19) Å

(b) C-S···π

3.4765(1) Å

3.4518(1) Å

(c) C-H···O

2.4857(1) Å

(d) C-H···B and C-H···F

3.0613(1) Å

2.5980(1) Å
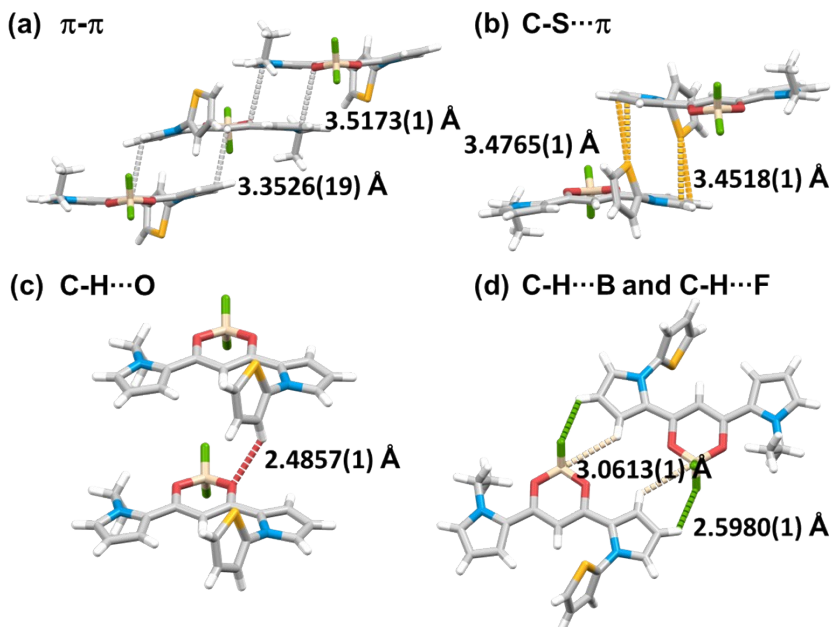
Figure S7. The intermolecular interactions in **G**. (a) π-π interactions, (b) C-S···π chalcogen bonds, (c) C-H···O hydrogen bonds and (d) C-H···B and C-H···F hydrogen bonds.

(a) π-π

3.3263(1) Å

3.2780(1) Å

(b) C-S···π

3.4410(1) Å

(c) C-H···F

2.4611(1) Å

(d) C-H···B and C-H···F

3.0248(1) Å   2.3759(1) Å
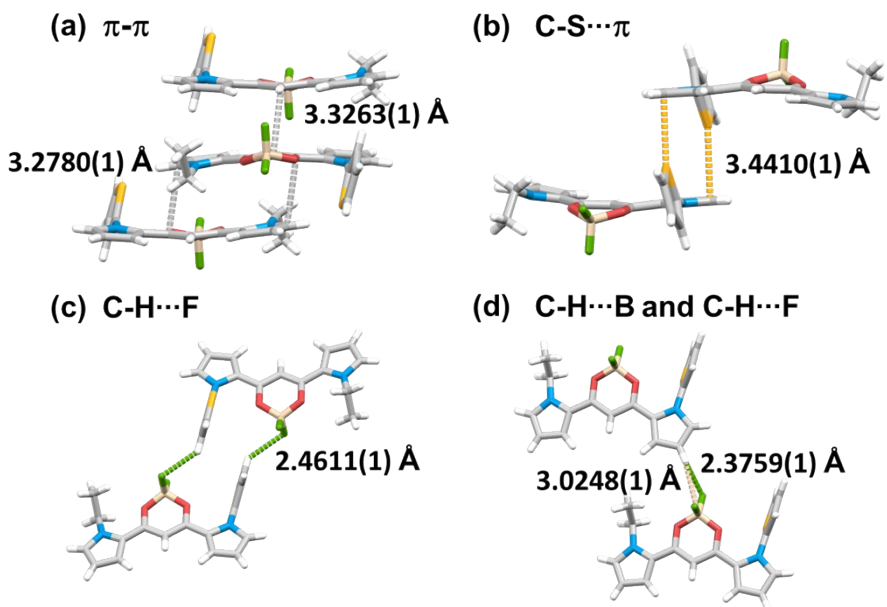
Figure S8. The intermolecular interactions in **O**. (a) π-π interactions, (b) C-S···π chalcogen bonds, (c) C-H···F hydrogen bonds and (d) C-H···B and another C-H···F hydrogen bonds.

Table S9. The torsion angles between different domains of **SNN**.
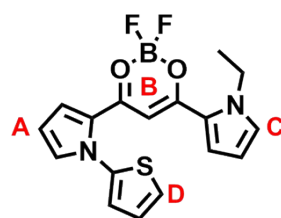
Torsion angle	A & B	B & C	D & A
G	9.2(2)°	9.2(2)°	66.40(16)°
O	5.902(3)°	11.716(3)°	74.495(4)°

Table S10. Photophysical data of **SNN** in solution and solid.

Samples	λ_{abs} (nm)	ε (cm^{-1}·M^{-1})	λ_{ex} (nm)	λ_{em} (nm)	τ_{em} (ns)	Φ (%)
Toluene solution	433	61347	435°	453	1.6	36
n-Hexane solution	422	51352	422	439	—	—
Tetrahydrofuran solution	433	61462	433	452	—	—
Dichloromethane solution	436	73390	436	460	—	—
Methanol solution	434	54531	434	458	—	—
1 wt% PMMA film	—	—	310	480	1.9	—
50 wt% PMMA film	—	—	310	577	13.8	—
G	—	—	365	514	0.8	21
O	—	—	365	592	23	16

8. Emission spectra in solid
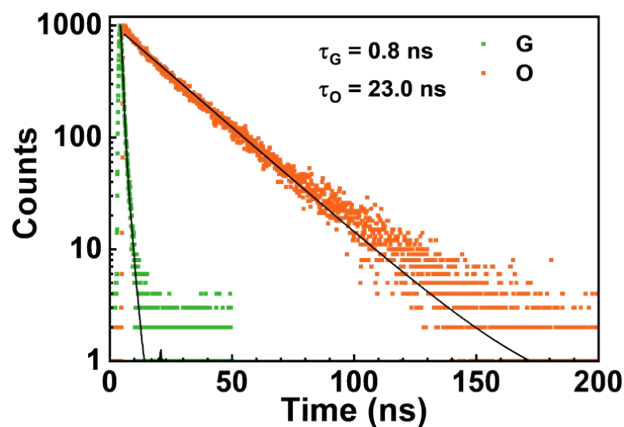
Figure S9. The fluorescence decay profiles **G** and **O**.
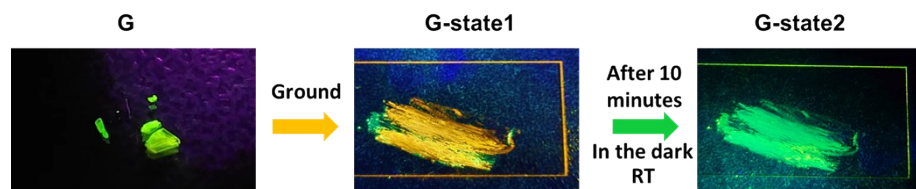
Figure S10. The images of **G**, **G-state1** and **G-state2**. The transformation from **G-state1** to **G-state2** occurs in the dark and at room temperature.
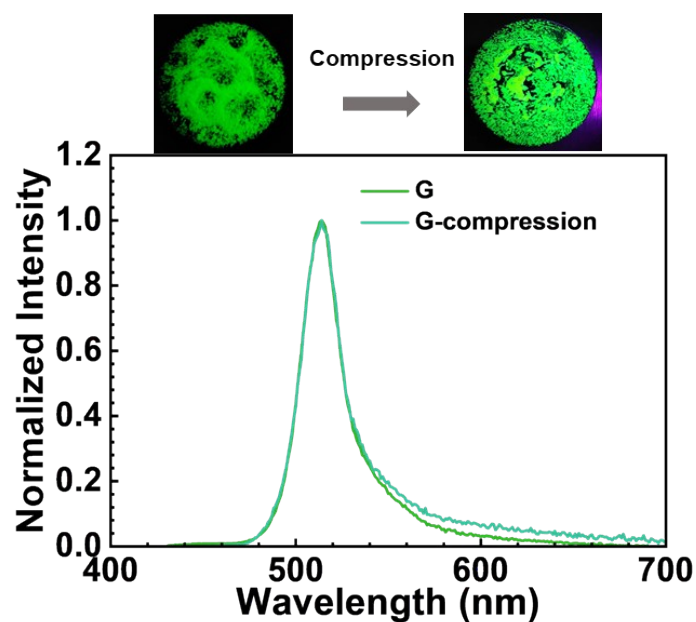

Figure S11. (a) The normalized fluorescence spectra of **G** and compression powder.
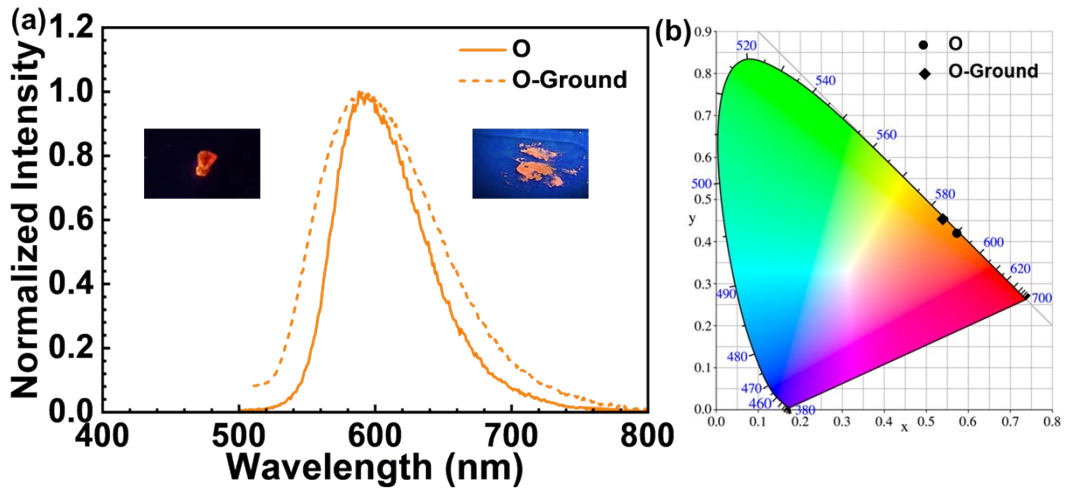
Figure S12. (a) The normalized fluorescence spectra and (b) CIE coordinate diagram of **O** crystals and ground powder.

8. Powder X-ray diffraction
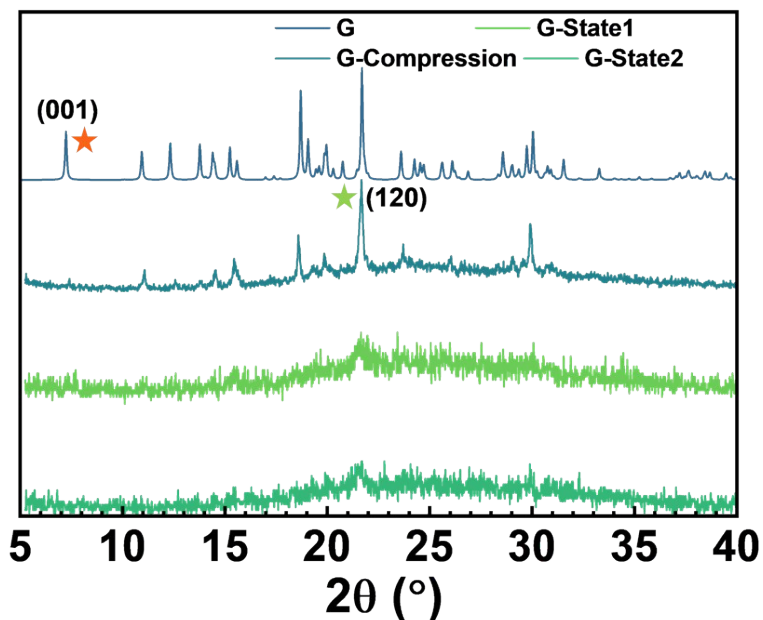
**Figure S13.** PXRD profiles of **SNN** in different state.
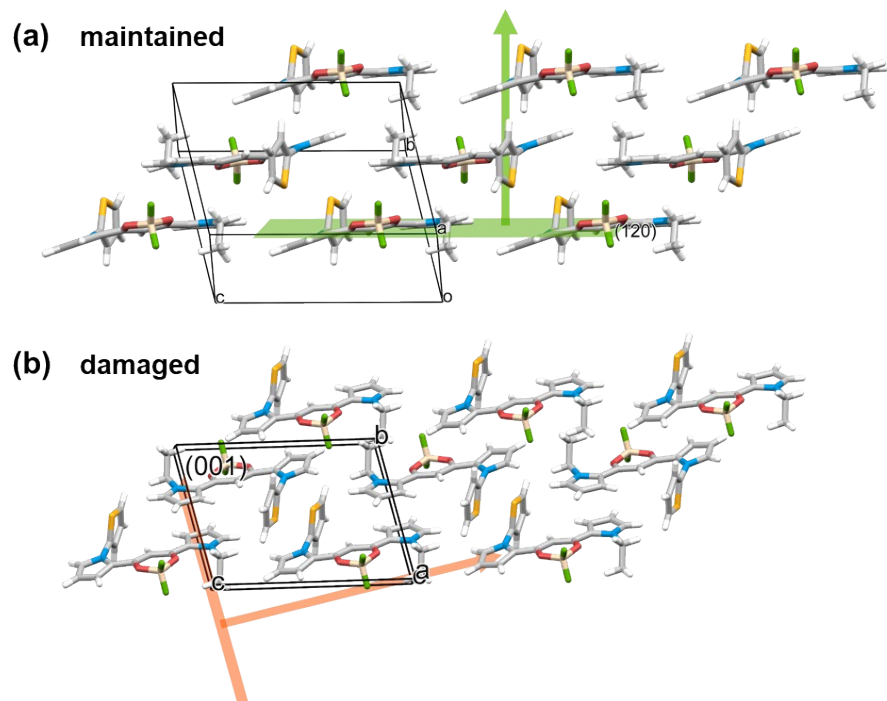
Figure S14. The structures of **G** along the directions perpendicular to the (a) (120) and (b) (001) plane. The (120) and (001) planes are drawn as a green plane and an orange plane. The arrows denote their vertical directions.

10. NMR spectra
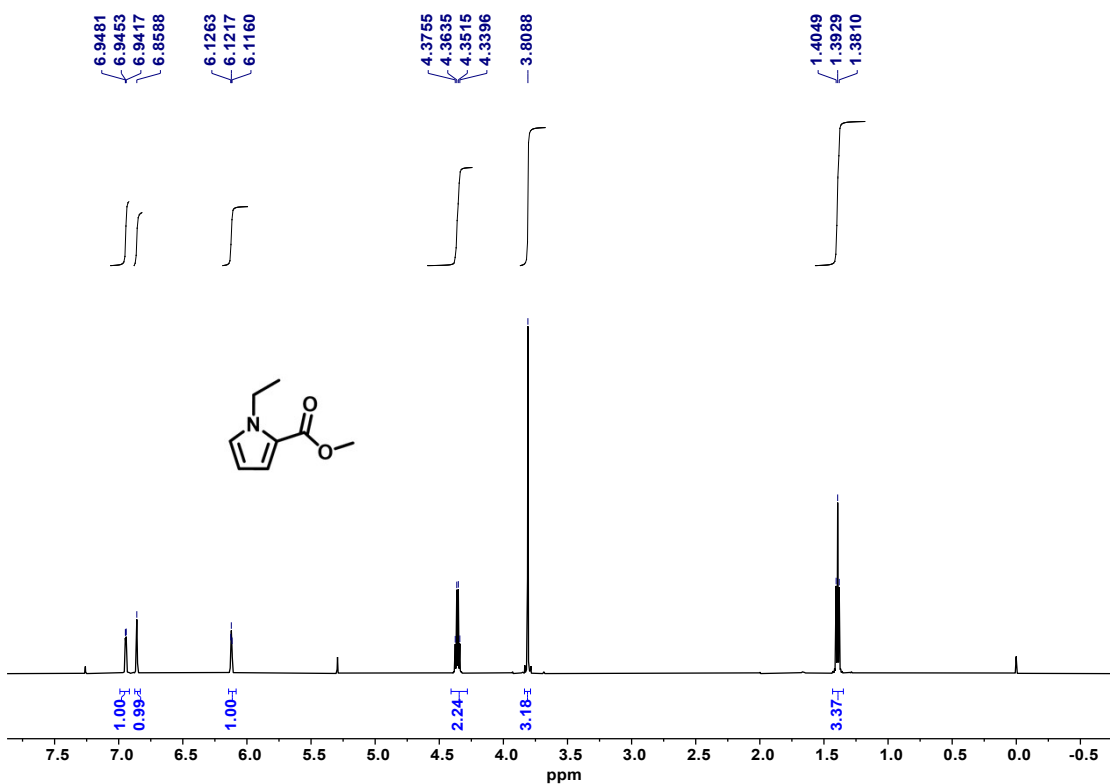
Figure S15. The ^{1}H NMR spectrum of compound **5** in CDCl$_3$ (600 MHz, 298 K).
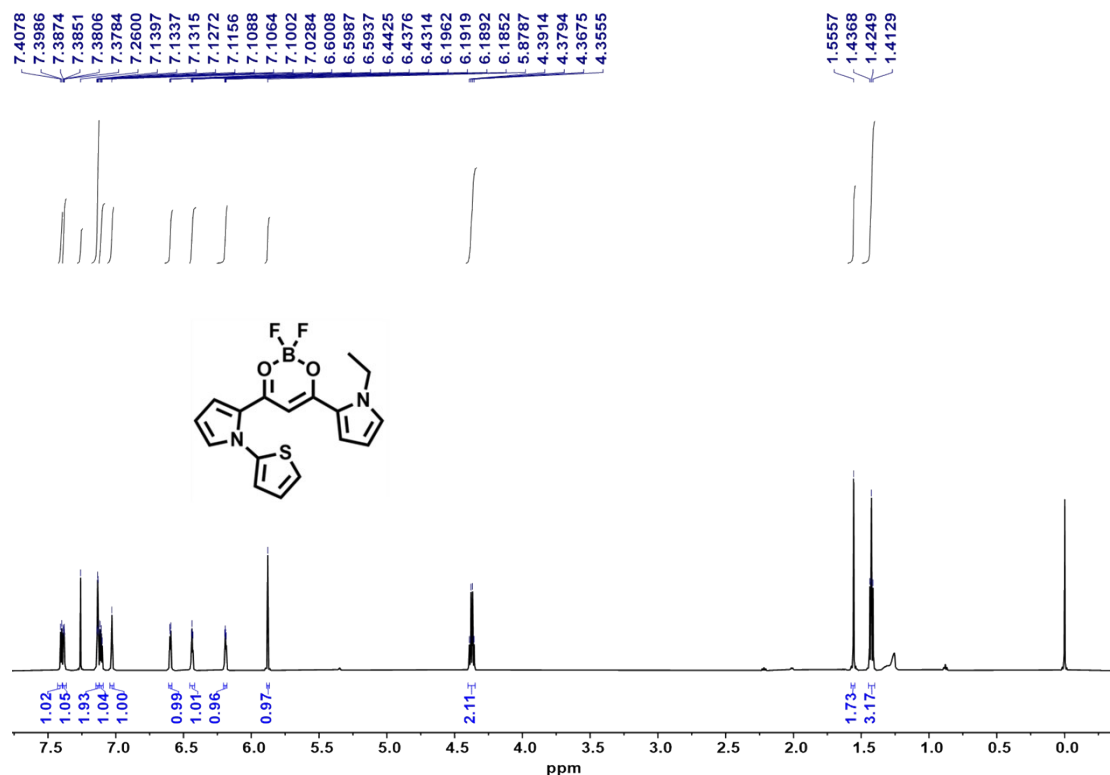
Figure S16. The ^{1}H NMR spectrum of **SNN** in CDCl$_3$ (600 MHz, 298 K).
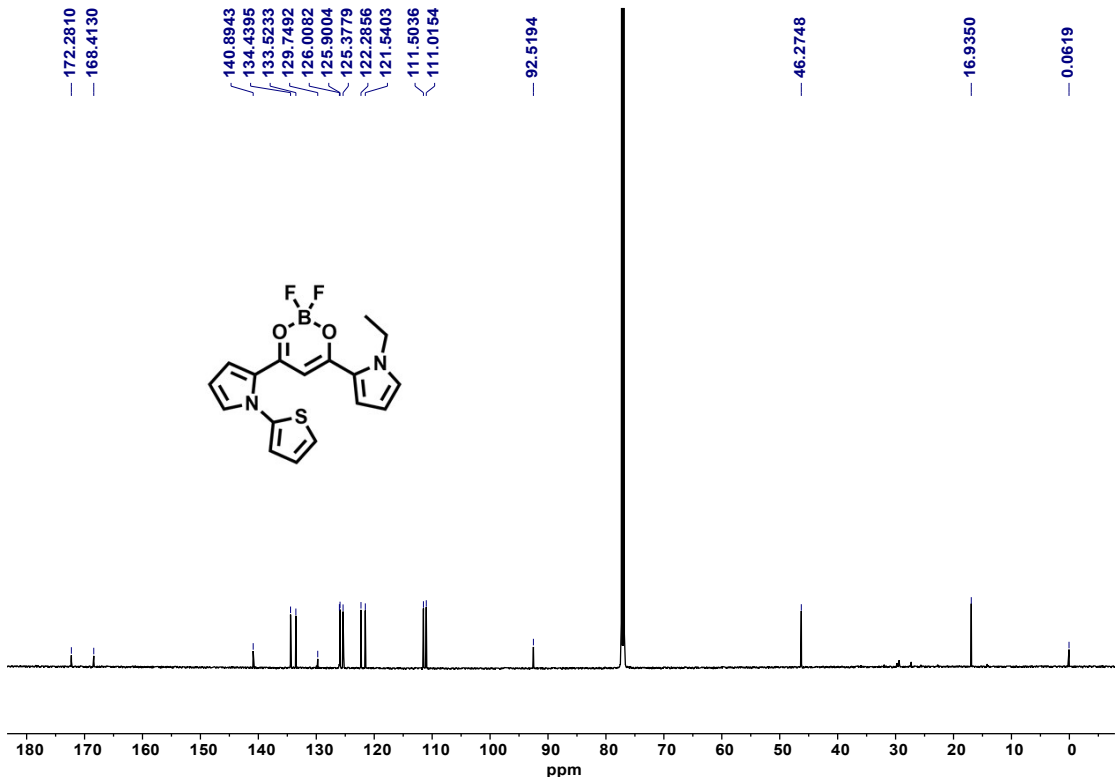
Figure S17. The ^{13}C NMR spectrum of **SNN** in CDCl$_3$ (600 MHz, 298 K).

11. Mass spectra
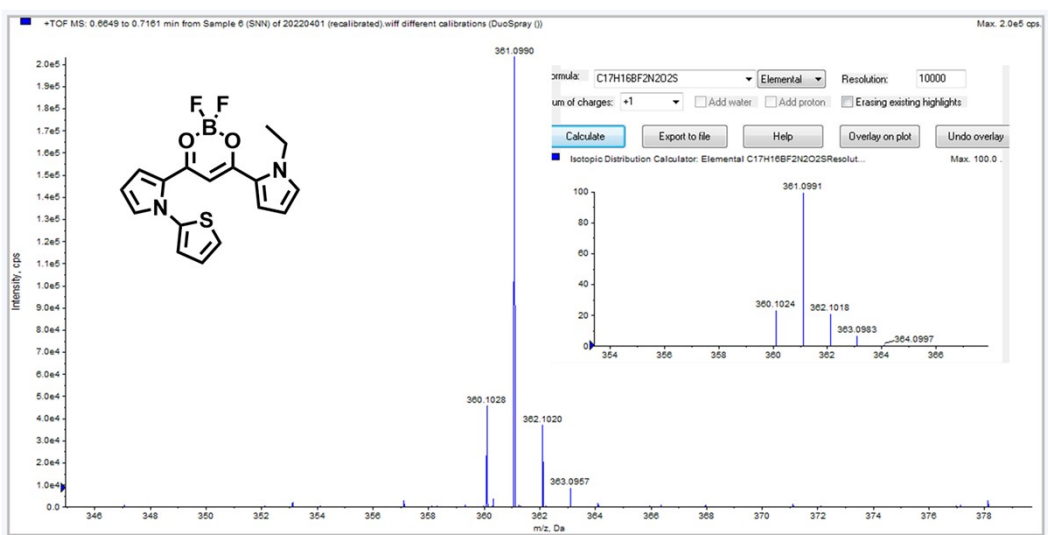
Figure S18. Calculated and experimental ESI-MS spectra of **SNN**.

14. References

1. F. Kleemiss, O. V. Dolomanov, M. Bodensteiner, N. Peyerimhoff, L. Midgley, L. J. Bourhis, A. Genoni, L. A. Malaspina, D. Jayatilaka, J. L. Spencer, F. White, B. Grundkotter-Stock, S. Steinhauer, D. Lentz, H. Puschmann and S. Grabowsky, *Chem. Sci.*, 2021,**12**, 1675–1692.

2. M. J. Frisch, G. W. Trucks, H. B. Schlegel, G. E. Scuseria, M. A. Robb, J. R. Cheeseman, G. Scalmani, V. Barone, B. Mennucci, G. A. Petersson, H. Nakatsuji, M. Caricato, X. Li, H. P. Hratchian, A. F. Izmaylov, J. Bloino, G. Zheng, J. L. Sonnenberg, M. Hada, M. Ehara, K. Toyota, R. Fukuda, J. Hasegawa, M. Ishida, T. Nakajima, Y. Honda, O. Kitao, H. Nakai, T. Vreven, J. A. Montgomery, Jr., J. E. Peralta, F. Ogliaro, M. Bearpark, J. J. Heyd, E. Brothers, K. N. Kudin, V. N. Staroverov, R. Kobayashi, J. Normand, K. Raghavachari, A. Rendell, J. C. Burant, S. S. Iyengar, J. Tomasi, M. Cossi, N. Rega, J. M. Millam, M. Klene, J. E. Knox, J. B. Cross, V. Bakken, C. Adamo, J. Jaramillo, R. Gomperts, R. E. Stratmann, O. Yazyev, A. J. Austin, R. Cammi, C. Pomelli, J. W. Ochterski, R. L. Martin, K. Morokuma, V. G. Zakrzewski, G. A. Voth, P. Salvador, J. J. Dannenberg, S. Dapprich, A. D. Daniels, Ö. Farkas, J. B. Foresman, J. V. Ortiz, J. Cioslowski, and D. J. Fox, Gaussian 09 (Gaussian, Inc., Wallingford CT, 2009).

3. Z.-F. Liu, J. Ren, P. Li, L.-Y. Niu, Q. Liao, S. Zhang and Q.-Z. Yang, *Angew. Chem. Int. Ed.*, 2022, e202214211.